Visualizing cellular interactions with a generalized proximity reporter

Mark A. Sellmyer[a,b], Laura Bronsart[b], Hiroshi Imoto[a], Christopher H. Contag[b,1], Thomas J. Wandless[a,1], and Jennifer A. Prescher[b,2]

[a]Department of Chemical and Systems Biology, and [b]Departments of Pediatrics, Radiology, and Microbiology and Immunology, Stanford University, Stanford, CA 94305

Edited by Carolyn R. Bertozzi, University of California, Berkeley, CA, and approved April 10, 2013 (received for review October 26, 2012)

Interactions among neighboring cells underpin many physiological processes ranging from early development to immune responses. When these interactions do not function properly, numerous pathologies, including infection and cancer, can result. Molecular imaging technologies, especially optical imaging, are uniquely suited to illuminate complex cellular interactions within the context of living tissues in the body. However, no tools yet exist that allow the detection of microscopic events, such as two cells coming into close proximity, on a global, whole-animal scale. We report here a broadly applicable, longitudinal strategy for probing interactions among cells in living subjects. This approach relies on the generation of bioluminescent light when two distinct cell populations come into close proximity, with the intensity of the optical signal correlating with relative cellular location. We demonstrate the ability of this reporter strategy to gauge cell–cell proximity in culture models in vitro and then evaluate this approach for imaging tumor–immune cell interactions using a murine breast cancer model. In these studies, our imaging strategy enabled the facile visualization of features that are otherwise difficult to observe with conventional imaging techniques, including detection of micrometastatic lesions and potential sites of tumor immunosurveillance. This proximity reporter will facilitate probing of numerous types of cell–cell interactions and will stimulate the development of similar techniques to detect rare events and pathological processes in live animals.

chemical biology | immunology | bioluminescence imaging | bioengineering | systems biology

Examining cells in their native context is crucial to understanding the biology of multicellular organisms. Cell motility, growth, and function are affected by interactions with neighboring cells and the surrounding microenvironment, and these features are difficult to recapitulate outside of the living organism. To detect molecular and cellular behaviors in their native contexts, optical imaging probes, such as the bioluminescent and fluorescent proteins, have proven particularly advantageous. These tools use nondestructive visible light and are compatible with most cell and tissue types (1, 2). In vivo bioluminescence imaging relies on enzymes (luciferases) that catalyze light emission using small-molecule substrates (luciferins), and favorable signal-to-noise ratios make it an especially sensitive bioassay in small living mammals. The emitted light can be detected using a CCD camera, and because no excitation light is required, there is virtually no background signal. Furthermore, the genetic encodability of luciferase(s) allows longitudinal experiments tracking signal over extended periods of time (3). The extraordinary sensitivity and broad dynamic range of bioluminescence are attractive features for in vivo imaging, and bioluminescence has been used for tracking cells in experiments affecting diverse areas of biology, including hematopoiesis and stem cell biology (4), tumor immunology (5), and bacterial pathogenesis (6).

Although constitutive expression of active bioluminescent proteins can provide sensitive, noninvasive readouts on the relative anatomical location of a cell population of interest, this alone cannot provide details about the particular cellular niche or tissue microenvironment, due, in part, to the low spatial resolution of whole-body optical imaging. Such approaches can therefore not be used for visualizing the most intricate cellular interactions, including the interaction of immune cells with tumor cells, a process important at both primary and metastatic sites (7). Intravital microscopy addresses the problem of limited resolution by placing a microscope objective into the animal and detecting fluorescently labeled cells (8). However, this technique only surveys a small, previously selected tissue sample and has limited ability to analyze the mobility and interactions of cells over extended time and distance scales (9).

To address the constraints of current methods for studying cell behavior in living animals, we developed a proximity reporter strategy for visualizing cell–cell interactions and demonstrate its utility in live animals. This approach uses the enzymatic catalysis and release of D-luciferin from one cell population for preferential use by a different, neighboring cell population; thus, the bioluminescent signal intensity is dependent on the distance between the two cell populations. In addition to characterizing the proximity reporter both in vitro and in vivo, we demonstrate that this approach improves the detection of metastases and immunosurveillance in a murine cancer model. Our method represents an important expansion of the molecular imaging toolkit because it addresses the need for longitudinal, noninvasive analyses of microscopic processes in living animals.

In the design of this strategy, we desired a tool with the following features: (*i*) a sensitive and dynamic readout of cell–cell proximity in live animals, (*ii*) widely accessible reagents and detection equipment, and (*iii*) potential for expansion of the platform. Thus, we were attracted to a well-described class of bioluminescent substrates, "caged" luciferins, that consist of a luciferin molecule covalently attached with a steric appendage (i.e., cage) that precludes binding of the molecule to luciferase. However, in the presence of enzymes capable of removing the cage, D-luciferin is liberated and available for the light-emitting reaction. Caged luciferins have been used for decades to measure enzymatic activities in vitro; most recently, they have been used to assay β-galactosidase (β-gal), β-lactamase, and alkaline phosphatase activities in cells (10–12) and live animals (13).

Here, we describe repurposing the caged luciferin technology to be a cell proximity reporter by genetically encoding β-gal, the uncaging enzyme, in one cell population (termed "activator" cells) and luciferase in another population (termed "reporter" cells) (Fig. 1*A*). We hypothesized that the activator cells (expressing

Author contributions: M.A.S., C.H.C., T.J.W., and J.A.P. designed research; M.A.S., L.B., and J.A.P. performed research; M.A.S., H.I., and J.A.P. contributed new reagents/analytic tools; M.A.S., L.B., C.H.C., T.J.W., and J.A.P. analyzed data; and M.A.S., C.H.C., T.J.W., and J.A.P. wrote the paper.

The authors declare no conflict of interest.

This article is a PNAS Direct Submission.

[1]To whom correspondence may be addressed. E-mail: ccontag@stanford.edu or wandless@stanford.edu.

[2]Present address: Departments of Chemistry and Molecular Biology and Biochemistry, University of California, Irvine, CA 92697.

This article contains supporting information online at www.pnas.org/lookup/suppl/doi:10.1073/pnas.1218336110/-/DCSupplemental.

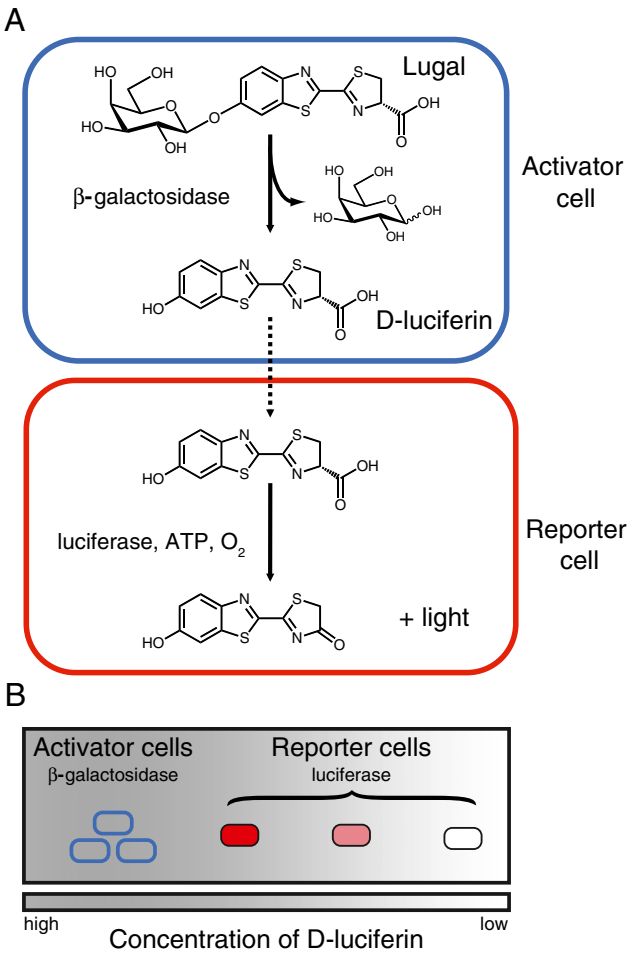

Fig. 1. Proximity reporter conceptual design. (*A*) Visualization of cell proximity with bioluminescent tools. Activator cells (expressing β-gal) catalyze the cleavage of Lugal, ultimately releasing D-luciferin. The liberated substrate enters nearby reporter cells, where it is used by luciferase to produce light. (*B*) General strategy for visualizing the relative location of two cell populations. Activator cells potentiate the release of D-luciferin. Neighboring reporter cells use the substrate to produce light. The concentration of D-luciferin is highest near the activator cells (indicated by gray-scale shading). As the distance between the reporter and activator cell decreases, light production increases (indicated by the red color).

β-gal) would catalyze the release of D-luciferin from the galactose-caged substrate Lugal and that D-luciferin would diffuse out of activator cells and into neighboring reporter cells (expressing luciferase) for light-emitting catalysis. Reporter cells nearest the activator cells would consume the most substrate, resulting in a correlation between the signal intensity and reporter cell and activator cell proximity (Fig. 1*B*). The β-gal–Lugal pair was chosen due to its low immunogenicity and toxicity, rapid kinetics, and potential to fulfill the general criteria listed above for proximity reporter development (10, 13).

Results and Discussion

Testing the Proximity Reporter in Vitro. To evaluate the proposed proximity reporter system, we first examined whether "uncaged" luciferin could diffuse out of the activator cells and be used by reporter cells in vitro. We incubated the substrate Lugal with activator HEK293 cells and assayed for luciferin release into the surrounding media. Lugal (100 μg/mL) was added to monolayers of control or activator HEK293 cells (1×10^4 cells per well) for 0–30 h. The media from the cells were then removed and transferred to reporter cells (1×10^4 cells per well). The resulting light emission was quantified using a CCD camera (IVIS; Fig. S1*A*). An approximate sevenfold increase in signal intensity was detected from reporter cells treated with media collected from activator cells relative to control cells within the first 15 min of incubation. Longer incubation times increased levels of background luminescence, likely the result of nonspecific hydrolysis of Lugal or endogenous β-gal activity within the HEK293 cells (14).

Second, we examined the effects of Lugal concentration on signal intensity. Lugal (1–500 μg/mL) was incubated with activator cells or control cells for 30 min, and the media were transferred to reporter cells (Fig. S1*B*). Again, an approximate eightfold increase in signal was observed even at low concentrations of Lugal (1 μg/mL). Higher concentrations of Lugal (500 μg/mL) resulted in an increase in background signal, suggesting nonspecific hydrolysis of Lugal to D-luciferin.

Third, we investigated the effect of β-gal levels on bioluminescent light production by varying the number of activator cells. Dilutions of activator cells were incubated with Lugal (100 μg/mL) for 30 min, and the media were transferred to plates containing reporter cells as above. A 1:10 ratio of activator:reporter cells provided a fivefold increase in signal above background (Fig. S1*C*). Collectively, these data indicate that substrate uncaging and diffusion are both rapid and constant over a wide range of Lugal concentrations, and that free luciferin can diffuse out of activator cells.

Although luciferin production by activator cells is both rapid and robust, real-time assessments of cell–cell proximity require that the liberated substrate be efficiently used by neighboring reporter cells. If luciferin builds up in the extracellular space or diffuses rapidly away from the site of production, any luciferase-expressing cell could use the substrate for light production, regardless of its proximity to the activator source. This scenario would limit our ability to correlate light production with spatial proximity. Conversely, insufficient production and/or liberation of D-luciferin by the activator cells would also be detrimental to our approach. Given these constraints, we examined whether the signal intensity correlated with the relative location and/or proximity of activator cells to reporter cells (i.e., cellular propinquity).

Visualizing Cell Proximity with Cultured Cell Models. We established a real-time cellular proximity assay using immobilized activator cells (Fig. 2*A*). Suspensions of control or activator cells in ECM (Matrigel; BD Bioscience) were placed in the middle of a 6-cm^2 tissue culture dish. The matrix was allowed to solidify before reporter cells were added in a monolayer surrounding the Matrigel. A β-gal assay confirmed the presence of active enzyme in activator cells (Fig. 2*B*). When human activator cells and mouse reporter cells were cultured together, a distinct border was visible by light microscopy, suggesting xenogenic chemorepulsion, which has been observed previously (15) (Fig. 2*C*). On addition of Lugal to this coculture (100 μg/mL for 1 h), the reporter cells nearest the activator cells exhibited the strongest light emission (Fig. 2*D*). Quantification of a cross-section of the image indicated a >20-fold induction of signal nearest the activator cells and a sharp reduction in signal over a 5-mm distance (Fig. 2*E*).

To assess whether the relative number of reporter cells in close proximity neighboring the activator cells in ECM influences the amount of signal produced, we diluted the number of reporter cells (100%, 50%, and 25%) in the coculture assay (Fig. S2). As anticipated, the signal intensity dropped sharply with dilution of reporter cells. Moreover, bioluminescence was not observed in the most dilute reporter cell-activator cell cocultures. These results are supported by a small-molecule diffusion model that suggests the reporter cells within 30 μm of activator cells (i.e., within several cell lengths) will have the highest signal production over a short time scale (1 h) (*SI Discussion*).

We further examined the proximity reporter using syngeneic cultures of activator and reporter cells. In this case, both cell populations

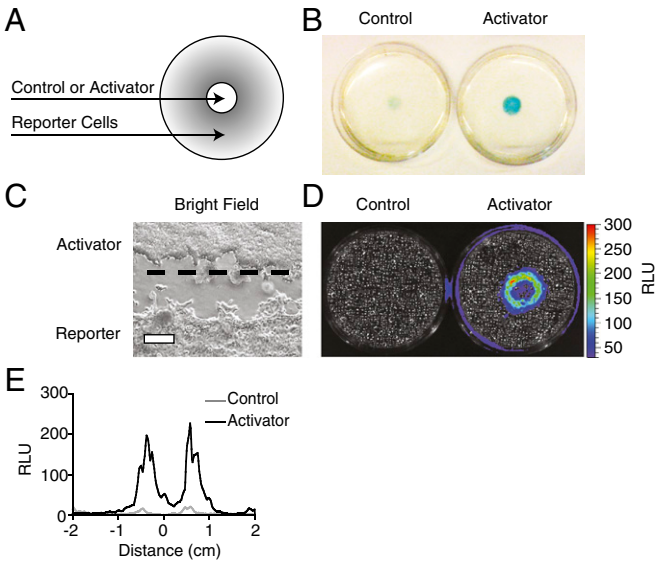

Fig. 2. Activator-reporter cell proximity visualized in vitro. (*A*) Schematic of coculture assay. Activator or control HEK293 cells (1×10^6 cells in Matrigel) were plated in the center of a 6-cm^2 dish (white circle). 4T1-luc2 reporter cells were plated in a monolayer surrounding the activator cells. The gray shading represents a possible distribution of luciferin (emanating from the activator cells) across the reporter cell zone, with darker shades corresponding to larger amounts of substrate. (*B*) Reporter cells surrounding either control (*Left*) or activator (*Right*) cells were incubated with X-gal for 4 h and imaged. The blue color correlates with β-gal activity. (*C*) Bright-field image of an activator-reporter cell coculture (Magnification: 10×.) HEK293 activator cells are located above the dashed line, and 4T1-luc2 reporter cells are located below the dashed line. (Scale bar: 40 μm.) (*D*) Representative bioluminescence image of cocultures after 48 h of incubation and subsequent incubation with Lugal. Each dish was incubated with Lugal (100 μg/mL) for 1 h before image acquisition. Light emission was measured in relative luminescent units (RLU) and correlates with reporter cell proximity to the activator cells. (*E*) Quantification of the light output from *D*. Photon counts along a 4-cm horizontal line through the center of each 6-cm^2 dish are plotted. The zero point corresponds to the center of the 6-cm^2 dish.

were HEK293 human cells and the reporter cells (labeled with a fluorescent protein) migrated into the matrix-immobilized activator cell region (Fig. S3*A*). When these cultures were treated with Lugal, a marked difference in signal production was observed relative to the xenogenic coculture. Rather than the ring pattern, the syngeneic cultures produced the strongest signal from within the matrix, indicative of reporter cells migrating into the matrix; this was confirmed by microscopy (Fig. S3 *B* and *C*). These data suggest that reporter cells within the matrix, in closest proximity to the activator cells, emitted the strongest signal and were the proof-of-principle before translating these in vitro experiments into animals.

Imaging Cell Proximity in Live Animals. We next evaluated the proximity reporter in live animals, where the diffusibility of the uncaged luciferin could have limited the utility of this approach. Large interstitial pressures or blood flow, two parameters not easily modeled in culture, could potentially distribute the substrate to tissues and regions quite distant from the site of origin (activator cells), impeding our ability to distinguish the relative locations of reporter cells. To examine whether two populations of cells could be spatially resolved in vivo, we implanted a mixed population of HEK293 activator and reporter cells in the upper left flank of immune-deficient (CD1 *nu/nu*) mice. These "coinjected" regions contained different ratios (10:1, 1:1, and 0.1:1) of activator and reporter cells (totaling 5×10^6–5×10^4:5×10^5 cells per graft). The control group contained untransduced HEK293 cells at a 10:1 ratio with reporter cells in the coinjected regions. A xenograft of reporter cells alone (5×10^5 cells) was placed at an "indicator" region in the contralateral hind flank. In this experiment, luciferin should be released in the coinjected regions and used preferentially by the reporter cells in that graft. If the more distant indicator regions produced strong signal, this would suggest that interstitial pressure, blood flow, or other fluid dynamics could rapidly distribute uncaged luciferin throughout the organism, limiting the utility of the proximity reporter for in vivo imaging of cellular propinquity.

Mice were imaged 5 min after i.p. injection of Lugal (1 d after engraftment) and then with luciferin on alternating days for 8 d. Bioluminescence signal produced in the coinjected regions was dose-dependent, with larger numbers of activator cells producing the most signal (Fig. 3*A* and *C*). Mice implanted with a 10:1 ratio of activator cells to reporter cells showed a >20-fold induction at the coinjected grafts relative to both the corresponding indicator region and the coinjected region of a control group on day 4. Luciferin was injected into all animals on day 5, and a similar number of luciferase-expressing reporter cells were indicated in all regions (Fig. 3*B*).

The signal intensity observed with the proximity reporter in vivo is likely attributable to three parameters: the number of activator cells; the number of reporter cells; and the surrounding tissue characteristics, including depth and overlying tissue type. Normalizing to luciferin signal removes reporter cell numbers and tissue characteristics from the variables affecting proximity reporter signal intensity. When we performed this normalization procedure, the 10:1 and 1:1 ratios of activator cells to reporter cells had roughly equivalent signal induction (Fig. S4*A*). The 0.1:1 group had threefold less than the other groups, suggesting that the signal intensity is dependent on the number of activator cells and that a 1:1 ratio

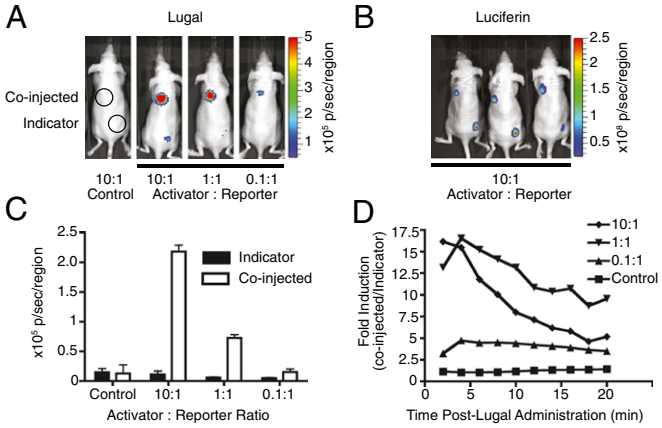

Fig. 3. Visualization of cell proximity in vivo. (*A*) Sample bioluminescence images from Lugal-treated animals. Mice ($n = 4$) were inoculated with mixed populations of activator (or control) and reporter cells (coinjected in upper left flank). Different ratios of activator/reporter cells were used in the coinjected regions (10:1, 1:1, and 0.1:1). Reporter cells (5×10^5) were held constant in all groups. The control group contained a 10:1 ratio of untransduced HEK293 cells with reporter cells. Reporter cells alone (5×10^5) were also implanted at a further distance from the activator cells (indicator in lower right flank). Mice were imaged daily for 8 d after treatment with Lugal (2 mg per mouse administered i.p.) or an equimolar amount of luciferin (1.3 mg per mouse administered i.p.) postcell implantation. (*B*) Sample bioluminescence images from animals treated with D-luciferin on day 5. Mice from the 10:1 activator/reporter cell (coinjected) cohort were injected with D-luciferin (1.3 mg per mouse administered i.p.) and imaged as before. Bioluminescence signal indicates the presence of luciferase-expressing reporter cells in both the coinjected and indicator regions. (*C*) Quantification of Lugal bioluminescence from coinjected regions on day 4 after cell implantation ($n = 4$). (*D*) Bioluminescence signal induction in coinjected region compared with indicator region ($n = 4$). All error bars represent the SEM for $n = 4$ mice. p, photons.

of cell types is likely to produce maximal signal induction. These data do not indicate that the proximity reporter provides absolute quantitation of activator and reporter cell numbers in a particular locale. Issues of tissue depth, overlying tissue type, and vascular supply may require experimental standardization for quantification of any bioluminescence reporter, and not just the proximity reporter (16). However, these data do indicate that the proximity reporter may direct investigators to sites of cellular interactions on a whole-animal scale.

The induction of bioluminescence signal in the coinjected regions relative to the indicator regions was highest at early time points after Lugal administration (1–5 min), suggesting that interaction sites may be rapidly identified after substrate administration (Fig. 3*D*). At later time points (5–20 min), however, the signal induction deceased due to increases in indicator region signal, especially in the 10:1 ratio experimental group. These data suggest that diffusion of the uncaged substrate to distant cells occurred over time, resulting in systemic distribution, and that reporter cells in these coinjected tumors were not able to catalyze all the uncaged substrate. Although this finding does not affect the functionality of the proximity reporter at early time points, it may affect experiments that require longer imaging times.

Additionally, the bioluminescence signal in coinjected and indicator regions steadily increased over 20 min after Lugal administration, indicating that Lugal is nonspecifically hydrolyzed in vivo as we previously observed in vitro (Fig. S4*B*). Nonspecific hydrolysis of Lugal is known to occur in mammals due to endogenous β-gal activity, and the covalent bond between the galactose moiety and luciferin in Lugal is especially prone to cleavage in solution (13).

Cell tracking with in vivo bioluminescence imaging follows one cell population over time; similarly, this strategy tracks cell–cell proximity over time (Fig. S5). The bioluminescent signal from coinjected and reporter regions in all mice decreased over several days, likely due to immune clearance of the xenografts (*nu/nu* mice retain some functions of innate immunity) (17). Representative mice were euthanized at the end of the imaging experiment, and coinjected grafts were cultured ex vivo to verify the presence of functional activator cells (Fig. S6).

Illuminating Metastatic Lesions with Proximity Reporter. As an initial demonstration of the utility of this system, we applied the proximity reporter to the visualization of metastatic disease in an animal model of breast cancer. Metastases represent the most deadly and least understood aspect of cancer; this is due, in part, to the lack of suitable animal models for studying early metastases or micrometastases (18). Additionally, metastases begin as rare events with very few numbers of cells; such events are difficult to study with conventional imaging tools. Consequently, most metastases in the clinical and animal models are detected at relatively late stages of invasion. Sites of early metastases, along with the immune or stromal cellular interactions responsible for such movements, remain poorly understood and, in some cases, highly controversial (18–21).

We envisioned using the proximity reporter to identify areas of early metastatic development and possible immune surveillance. This experiment was designed to illuminate small numbers of reporter cells in close proximity to activator cells after invading into tissues distant from the primary tumor (Fig. S7). In our model system, irradiated immunodeficient mice were given an allograft of activator β-gal–expressing or control hematopoietic cells, and they were then given an orthotopic implant of luciferase-expressing metastatic breast cancer cells (Fig. 4*A*). The β-gal activity of the bone marrow cells was assessed using fluorescein-di-β-D-galactopyranoside (FDG) flow cytometry before transplantation (Fig. S8*A*), and bone marrow reconstitution was successful by 3 wk posttransplantation (Fig. S8*B*). At the 7-wk experimental end point, a similar percentage of activator cells was found in the primary tumor and pulmonary parenchyma, suggesting a relatively equal distribution of transplanted cells in nonhematopoetic tissues (22) (Fig. 4*B*). These data also suggest that the engraftment percentage was similar in each animal.

Mouse breast carcinoma 4T1-luc2 reporter tumor cells (1×10^4) were implanted in the mammary fat pads of all mice 3 wk after bone marrow transplantation. Tumor engraftment was monitored with bioluminescence imaging, and palpable tumors arose by day 7. Mice were then injected with Lugal to visualize metastatic sites. During the same imaging session, the mice were subsequently injected with luciferin to ensure anatomical consistency for quantification of light emission and normalization for the number of reporter cells.

In our metastatic model, some metastases were enhanced by the proximity reporter, whereas others were not. For example, the nasal area of mouse 3 in cage 2 and a submandibular lymph node of mouse 5 in cage 2 were identified repeatedly as potential sites of immune–metastatic interaction indicated by an elevated Lugal-to-luciferin ratio (Fig. 4*C* and Fig. S9, arrows). The nasal metastasis was missed using conventional luciferin imaging; the entire dataset for this experiment is shown (Fig. S9). Ex vivo imaging of biopsied tissues confirmed the presence of reporter cells (Fig. S10*A*). Image-guided biopsies were assayed by X-gal histology and FDG flow cytometry. These assays confirmed the presence of activator cells in the biopsy sites (Fig. S10 *B* and *C*). Interestingly, there was not an elevated percentage of activator cells in the nasal area compared with the other metastatic sites. This suggests that these were true sites of activator-reporter proximity rather than an incidentally high signal based on the high number of immune cells in the nasal vault. Ultimately, conventional luciferin imaging draws attention toward the brightest metastasis, whereas proximity reporter imaging can show investigators potential sites of metastatic–immune cell interaction on a whole-animal scale.

Conclusions

Optical imaging tools are uniquely suited to address questions pertaining to cellular interactions in living animals. To date, most optical probes have been limited to monitoring microscopic features across short lengths or in superficial sites accessible to large-bulk optics of conventional confocal microscopes (via fluorescence) (23, 24). To expand on these capabilities and gain information about cellular interactions across larger length and time scales, we designed a unique imaging strategy that comprises a cell–cell proximity reporter. This system relies on the local uncaging of a bioluminescent substrate (luciferin) by activator cells and its utilization by a light-emitting enzyme (luciferase) expressed in reporter cells. Reporter cells nearest the activator cells use the most luciferin; thus, signal is generated only when these two cell populations are in close proximity.

Our data demonstrate that the proximity reporter can be used to resolve cellular interactions spatially in both cultured cells and live animals. The uncaging reaction catalyzed by the activator cells is rapid, and luciferin can diffuse out of activator cells. Neighboring reporter cells can preferentially catalyze the liberated substrate and can detect low numbers of activator cells with the addition of low levels of substrate. In both in vitro and in vivo models, the proximity-dependent signal is sensitive on a short, experimentally facile time scale and exhibits a robust, dynamic range (~20-fold in vivo) that correlates with the local concentration of activator cells. The proximity-dependent signal generated with Lugal was approximately two orders of magnitude less intense than traditional luciferin imaging. This suggests that at least 1,000 interacting reporter cells must be present in areas with sufficient activator cell activity to produce detectable signal (25). We do not suggest that the proximity reporter can provide absolute numbers of interacting cells; rather, we believe our method can serve as a guide for subsequent analyses. In other words, our proximity reporter will tell investigators where to look using existing, more detailed ex vivo methods.

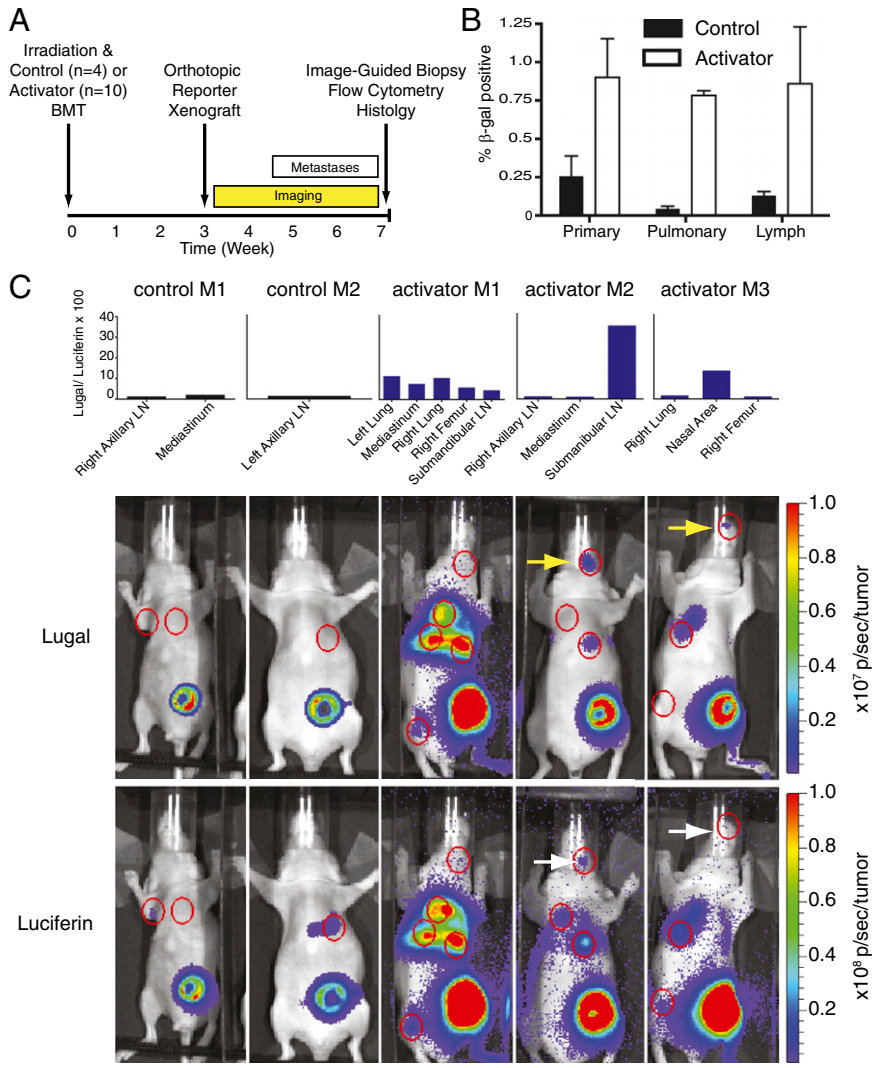

Fig. 4. Imaging tumor-immune cell propinquity. (*A*) Experimental design. Immunodeficient mice (*nu/nu*) were irradiated, and bone marrow was transplanted from β-gal–expressing transgenic mice, activator, or control mice. Three weeks after bone marrow transplantation (BMT), 4T1-luc2 reporter mammary carcinoma cells (1×10^4) were orthotopically allografted into the mammary fat pads of all animals. Metastases development in weeks 5–7 was monitored via bioluminescence imaging with Lugal and D-luciferin. End points were biopsy, flow cytometry, and histology. (*B*) Percentage of β-gal–expressing cells from image-guided biopsies of metastases in tumor, lung, and lymphatic tissues using FDG and flow cytometry. Error bars represent the SEM for $n \geq 3$ mice. (*C*) Proximity reporter imaging 29 d after tumor inoculation identifies potential sites of tumor–immune cell interactions. Images acquired with Lugal indicate sites of metastasis (red circles) in mice transplanted with control or activator cells ($n = 4$ and $n = 10$, respectively). Lugal (2 mg per mouse) was injected, and mice were imaged 5 min after i.p. injection. Yellow arrows indicate tumors that exhibit an elevated ratio of Lugal to D-luciferin in a submandibular lymph node (LN) of mouse 2 and the nasal area of mouse 3. After 10 min, luciferin (1.33 mg per mouse) was injected i.p. into the anesthetized animals in the imaging system. White arrows indicate the same metastases after subsequent D-luciferin injection. Histograms above the mice show the ratio of signal from Lugal to luciferin for each documented metastases. (Magnification: 100×.)

Although established models of cell–cell interaction could be assayed using the proximity reporter (5), we developed a cancer model to address the current challenge of identifying potential sites of metastatic immune surveillance. The proximity reporter was able to illuminate micrometastatic disease in this model. The identified metastatic sites showing enhanced proximity reporter signal, the nasal area and a submandibular lymph node, are not traditional sites visualized using bioluminescence imaging after an orthotopic allograft but are very possible sites of aggressive breast cancer metastasis (25, 26). Once sites of possible interaction are located, experiments can be performed that may provide insight into how metastatic cells escape or incite early immune recognition in that particular niche. Future experiments aimed at characterizing the types of cells and signaling pathways involved may enhance our understanding of micrometastasis development and help identify new therapies to combat this aspect of the disease.

This work lays the foundation for visualizing cellular proximity and interactions in a variety of biological settings. Many physiological processes, such as adaptive immunity or stem cell niche development, could be better understood using molecular tools that report the proximity of two cell populations. The proximity reporter is easily translatable to these areas, and the reagents and imaging tools are already widely in use. For example, it is not necessary to use two orthotopic or xenogenic cell lines to utilize the proximity reporter. Many commercially available transgenic mice that express β-gal and luciferase can be mated, producing offspring that express the enzymes in selective endogenous tissues or in response to physiologically relevant stimuli. Another exciting application involves illuminating sites of host–pathogen

interactions. Discovering when and where the specific immune cells arrive and interact with the bacteria would advance our understanding of sepsis and other deadly aspects of infection.

Additional efforts will be directed at developing orthogonal uncaging enzyme-substrate pairs, such as nitroreductase or herpes simplex virus thymidine kinase, and spectrally resolved luciferases, thereby enabling the potential visualization of multicellular networks (27, 28). Further improvements in signal-to-noise ratios may be obtained using more chemically stable caged luciferins or different enzyme-caged substrate pairs. Collectively, these tools will usher in a new era for in vivo imaging, allowing the observation and dissection of cell interactions in their most relevant, natural context.

Materials and Methods

Cell Culture and Transductions. HEK293 cells (American Type Cell Culture) and 4T1-luc2 cells (Caliper LifeSciences, now Perkin–Elmer) were cultured as described in *SI Materials and Methods*. β-Gal–expressing HEK293 cells (activator cells) were made by introducing a β-gal/β-lactamase fusion gene expressed from pcDNA6.2 Geneblazer iBlasticidin (Invitrogen) via cationic lipid transfection (Lipofectamine 2000; Invitrogen).

Lugal. Lugal was synthesized as previously reported (29) or obtained commercially from Promega (P1061).

In Vitro Cellular Proximity Assays. The experimental details describing all the cell-based assays (time course assay, Lugal dose–response assay, and activator cell saturation assay) are provided in *SI Materials and Methods*.

Cellular Coculture Assays. Experimental details describing the cell-based experiments and the subsequent imaging are provided in *SI Materials and Methods*.

Mouse Models. Descriptions of the experiments involving CD1 *nu/nu* mice to evaluate the proximity reporter, as well as the metastatic model, are provided in *SI Materials and Methods*. All animal studies were completed with Institutional Animal Care and Use Committee approval (Stanford University Protocols 12323 and 22936).

ACKNOWLEDGMENTS. We thank Drs. Yuan Cao, Michael Bachmann, and Tobi Schmidt for comments regarding this work. This work was supported by the US National Institutes of Health (NIH) through Grant GM073046 (to T.J.W.) and In Vivo Cellular and Molecular Imaging Center Grant P50 CA114747 (to C.H.C.). M.A.S. was supported by the NIH Medical Scientist Training Program, and J.A.P. was supported by fellowships from the Susan G. Komen Foundation and the Stanford Molecular Imaging Scholars Program.

1. Prescher JA, Contag CH (2010) Guided by the light: Visualizing biomolecular processes in living animals with bioluminescence. *Curr Opin Chem Biol* 14(1):80–89.
2. Gheysens O, Gambhir SS (2005) Studying molecular and cellular processes in the intact organism. *Prog Drug Res* 62:117–150.
3. Contag CH (2007) In vivo pathology: Seeing with molecular specificity and cellular resolution in the living body. *Annu Rev Pathol* 2:277–305.
4. Cao YA, et al. (2004) Shifting foci of hematopoiesis during reconstitution from single stem cells. *Proc Natl Acad Sci USA* 101(1):221–226.
5. Thorne SH, Negrin RS, Contag CH (2006) Synergistic antitumor effects of immune cell-viral biotherapy. *Science* 311(5768):1780–1784.
6. Hardy J, et al. (2004) Extracellular replication of Listeria monocytogenes in the murine gall bladder. *Science* 303(5659):851–853.
7. Teng MW, Swann JB, Koebel CM, Schreiber RD, Smyth MJ (2008) Immune-mediated dormancy: An equilibrium with cancer. *J Leukoc Biol* 84(4):988–993.
8. Zhao W, et al. (2011) Cell-surface sensors for real-time probing of cellular environments. *Nat Nanotechnol* 6(8):524–531.
9. Germain RN, Robey EA, Cahalan MD (2012) A decade of imaging cellular motility and interaction dynamics in the immune system. *Science* 336(6089):1676–1681.
10. Geiger R, Schneider E, Wallenfels K, Miska W (1992) A new ultrasensitive bioluminogenic enzyme substrate for beta-galactosidase. *Biol Chem Hoppe Seyler* 373(12):1187–1191.
11. Yao H, So MK, Rao J (2007) A bioluminogenic substrate for in vivo imaging of beta-lactamase activity. *Angew Chem Int Ed Engl* 46(37):7031–7034.
12. Zhou W, et al. (2006) New bioluminogenic substrates for monoamine oxidase assays. *J Am Chem Soc* 128(10):3122–3123.
13. Wehrman TS, von Degenfeld G, Krutzik PO, Nolan GP, Blau HM (2006) Luminescent imaging of beta-galactosidase activity in living subjects using sequential reporter-enzyme luminescence. *Nat Methods* 3(4):295–301.
14. Gong H, et al. (2009) beta-Galactosidase activity assay using far-red-shifted fluorescent substrate DDAOG. *Anal Biochem* 386(1):59–64.
15. Vianello F, Olszak IT, Poznansky MC (2005) Fugetaxis: Active movement of leukocytes away from a chemokinetic agent. *J Mol Med (Berl)* 83(10):752–763.
16. Berger F, Paulmurugan R, Bhaumik S, Gambhir SS (2008) Uptake kinetics and biodistribution of 14C-D-luciferin—A radiolabeled substrate for the firefly luciferase catalyzed bioluminescence reaction: Impact on bioluminescence based reporter gene imaging. *Eur J Nucl Med Mol Imaging* 35(12):2275–2285.
17. Herberman RB, Holden HT (1978) Natural cell-mediated immunity. *Adv Cancer Res* 27:305–377.
18. Hanahan D, Weinberg RA (2011) Hallmarks of cancer: The next generation. *Cell* 144(5):646–674.
19. Karnoub AE, et al. (2007) Mesenchymal stem cells within tumour stroma promote breast cancer metastasis. *Nature* 449(7162):557–563.
20. Dunn GP, Bruce AT, Ikeda H, Old LJ, Schreiber RD (2002) Cancer immunoediting: From immunosurveillance to tumor escape. *Nat Immunol* 3(11):991–998.
21. Bissell MJ, Kenny PA, Radisky DC (2005) Microenvironmental regulators of tissue structure and function also regulate tumor induction and progression: The role of extracellular matrix and its degrading enzymes. *Cold Spring Harb Symp Quant Biol* 70:343–356.
22. Krause DS, et al. (2001) Multi-organ, multi-lineage engraftment by a single bone marrow-derived stem cell. *Cell* 105(3):369–377.
23. Feinberg EH, et al. (2008) GFP Reconstitution Across Synaptic Partners (GRASP) defines cell contacts and synapses in living nervous systems. *Neuron* 57(3):353–363.
24. Shu X, et al. (2009) Mammalian expression of infrared fluorescent proteins engineered from a bacterial phytochrome. *Science* 324(5928):804–807.
25. Kim J-B, et al. (2010) Non-invasive detection of a small number of bioluminescent cancer cells in vivo. *PLoS ONE* 5(2):e9364.
26. Pulaski BA, Ostrand-Rosenberg S (2001) Mouse 4T1 breast tumor model. *Curr Protoc Immunol*, Chapter 20:Unit 20.2.
27. Bhaumik S, Sekar TV, Depuy J, Klimash J, Paulmurugan R (2012) Noninvasive optical imaging of nitroreductase gene-directed enzyme prodrug therapy system in living animals. *Gene Ther* 19(3):295–302.
28. Mailly L, Leboeuf C, Tiberghien P, Baumert T, Robinet E (2010) Genetically engineered T-cells expressing a ganciclovir-sensitive HSV-tk suicide gene for the prevention of GvHD. *Curr Opin Investig Drugs* 11(5):559–570.
29. Amess R, Baggett N, Darby PR, Goode AR, Vickers EE (1990) Synthesis of luciferin glycosides as substrates for novel ultrasensitive enzyme assays. *Carbohydr Res* 205: 225–233.